



# Application of the Kurganov–Levy semi-discrete numerical scheme to hyperbolic problems with nonlinear source terms

R. Naidoo<sup>a,b</sup>, S. Baboolal<sup>b,\*</sup>

<sup>a</sup> Department of Mathematics and Physics, Durban Institute of Technology, P.O. Box 1334, Durban 4000, South Africa

<sup>b</sup> Department of Computer Science, University of Durban-Westville, Private Bag X54001, Durban 4000, South Africa

---

## Abstract

In this paper are outlined the details required in adapting the third-order semi-discrete numerical scheme of Kurganov and Levy [SIAM J. Sci. Comput. 22 (2000) 1461] to handle hyperbolic systems which include source terms. The performance of the scheme is then assessed against a fully discrete scheme, as well as against reference solutions on problems such as shock propagation in a Broadwell gas and shocks in an Eulerian gas with heat transfer.

© 2003 Elsevier B.V. All rights reserved.

*Keywords:* Hyperbolic systems; Semi-discrete scheme; Shock capturing

---

## 1. Introduction

The problem of concern in this work is the numerical integration of

$$\frac{\partial u(x, t)}{\partial t} + \frac{\partial f(u(x, t))}{\partial x} = g(u(x, t)), \quad (1)$$

a one-dimensional hyperbolic system of partial differential equations. Here  $u(x, t)$  is the unknown  $m$ -dimensional vector function,  $f(u)$  the flux vector,  $g(u)$  a continuous source vector function on the right hand side (RHS), with  $x$  the single spatial coordinate and  $t$  the temporal coordinate. Further, in the applications to follow we shall allow for the RHS the form  $(1/\varepsilon)g(u(x, t))$ , where the parameter  $\varepsilon > 0$  distinguishes between stiff systems ( $\varepsilon \ll 1$ ) and standard, non-stiff ones ( $\varepsilon = 1$ ).

Such equations can be used to model many physical systems, including fluids and various types of gases. In the last decade, particularly following the work of Nessyahu and Tadmor [1], a family of fully discrete, high-resolution, Riemann-solver-free schemes have been produced in order to numerically solve hyperbolic systems such as the aforementioned. More recently, also based on the same Riemann-solver-free approach, second and third-order semi-discrete schemes were devised by Kurganov and Tadmor [2] and Kurganov and Levy [3]. One advantage of the latter is that they can be applied on non-staggered grids and thus ease the implementation of boundary conditions. Here we are particularly interested in the details of adapting the latter so that it be can applied to systems with source terms including those that are stiff. In order to assess the performance of this scheme we examine its merits against an adaptation [4] following [5] for non-staggered grids, of the fully discrete scheme of [1] for systems with source terms, as well as against exact or reference solutions for two prototype problems. One such is the problem of

---

\* Corresponding author. Tel.: +27-31-2044897; fax: +27-31-2044001.

*E-mail addresses:* sbab@pixie.udw.ac.za (S. Baboolal), naidoo@yoda.cs.udw.ac.za (R. Naidoo).

shock propagation in a Broadwell gas [6,7] and the other is that of shocks in a gas dynamics model with heat transfer.

## 2. The modified numerical scheme

### 2.1. Kurganov–Levy scheme for nonlinear source term

Here the numerical integration of problem (1) is considered on some uniform spatial and temporal grids with the spacings,  $\Delta x = x_{j+1} - x_j$ ;  $\Delta t = t^{n+1} - t^n$  (with  $j$  and  $n$  being suitable integer indices).

For the nonlinear homogeneous case of (1), Kurganov and Levy [3] obtain the third-order semi-discrete scheme:

$$\begin{aligned} \frac{d\bar{u}_j}{dt} = & -\frac{1}{2\Delta x} [f(u_{j+1/2}^+(t)) + f(u_{j+1/2}^-(t)) \\ & - f(u_{j-1/2}^+(t)) - f(u_{j-1/2}^-(t))] \\ & - \frac{a_{j+1/2}(t)}{2\Delta x} [u_{j+1/2}^+(t) - u_{j+1/2}^-(t)] \\ & - \frac{a_{j-1/2}(t)}{2\Delta x} [u_{j-1/2}^+(t) - u_{j-1/2}^-(t)], \end{aligned} \quad (2)$$

where

$$\begin{aligned} a_{j\pm 1/2}^n & \\ = \max & \left( \rho \left( \frac{\partial f}{\partial u} (u_{j\pm 1/2}^-(t)) \right), \rho \left( \frac{\partial f}{\partial u} (u_{j\pm 1/2}^+(t)) \right) \right) \end{aligned} \quad (3)$$

and

$$\begin{aligned} u_{j\pm 1/2}^+ & := P_{j+1}(x_{j\pm 1/2}, t^n), \\ u_{j\pm 1/2}^- & := P_j(x_{j\pm 1/2}, t^n). \end{aligned} \quad (4)$$

In the above, the forms (4) are, respectively, the left and right intermediate values at  $x_{j\pm 1/2}$  of a piecewise polynomial interpolant  $P_j(x, t^n)$  that fit an already computed or known cell average values  $\{\bar{u}_j^n\}$  at time level  $n$ . Also  $\rho(\cdot)$  denotes the spectral radius of the respective Jacobian, defining the maximum local propagation speeds  $a_{j\pm 1/2}^n$ .

They also obtain an extension of the above when the RHS of (1) is of the form  $\partial Q/\partial x$  where  $Q(u(x, t), u_x(x, t))$  is a dissipation flux satisfying a parabolicity condition [3].

However, to allow for a source term  $g(u(x, t))$  in (1) we must proceed as outlined in [3] and follow through the construction of the scheme with this added detail. Thus, employing the above mentioned uniform spatial and temporal grids and integrating (1) over the cell  $I(x) := \{\xi \mid |\xi - x| \leq \Delta x/2\}$  gives

$$\begin{aligned} \bar{u}_t + \frac{1}{\Delta x} \left[ f \left( u \left( x + \frac{\Delta x}{2}, t \right) \right) \right. \\ \left. - f \left( u \left( x - \frac{\Delta x}{2}, t \right) \right) \right] = \bar{g}, \end{aligned} \quad (5)$$

where

$$\bar{u}(x, t) := \frac{1}{\Delta x} \int_{I(x)} u(\xi, t) d\xi \quad (6)$$

and

$$\bar{g} := \frac{1}{\Delta x} \int_{I(x)} g(u(\xi, t)) d\xi. \quad (7)$$

Now assuming the  $\{\bar{u}_j^n\}$  are already computed or known cell averages of the approximate solution at time  $t = t^n$  we integrate as in [3] over the control volumes  $[x_{j-1/2,R}^n, x_{j-1/2,L}^n] \times [t^n, t^{n+1}]$ ,  $[x_{j-1/2,R}^n, x_{j+1/2,L}^n] \times [t^n, t^{n+1}]$  and  $[x_{j+1/2,L}^n, x_{j+1/2,R}^n] \times [t^n, t^{n+1}]$  where

$$\begin{aligned} x_{j\pm 1/2,L}^n & := x_{j\pm 1/2} - a_{j\pm 1/2}^n \Delta t, \\ x_{j\pm 1/2,R}^n & := x_{j\pm 1/2} + a_{j\pm 1/2}^n \Delta t \end{aligned} \quad (8)$$

with the piecewise polynomial form in the cell  $I_j$  taken as

$$P_j(x, t^n) = A_j + B_j(x - x_j) + \frac{1}{2}C_j(x - x_j)^2, \quad (9)$$

where the constants  $A_j, B_j, C_j$  are evaluated as in [3]. These then result, respectively, in the weighted averages  $\bar{w}_{j-1/2}^{n+1}, \bar{w}_j^{n+1}, \bar{w}_{j+1/2}^{n+1}$  which differ from those in [3] only in the respective additive source terms:

$$\frac{1}{2a_{j-1/2}^n \Delta t} \int_{x_{j-1/2,L}^n}^{x_{j-1/2,R}^n} \int_{t^n}^{t^{n+1}} g \, dx \, dt, \quad (10)$$

$$\frac{1}{\Delta x - \Delta t(a_{j-1/2}^n + a_{j+1/2}^n)} \int_{x_{j-1/2,R}^n}^{x_{j+1/2,L}^n} \int_{t^n}^{t^{n+1}} g \, dx \, dt \quad (11)$$

and

$$\frac{1}{2a_{j+1/2}^n \Delta t} \int_{x_{j+1/2,L}}^{x_{j+1/2,R}} \int_{t^n}^{t^{n+1}} g \, dx \, dt. \quad (12)$$

Then from the cell averages  $\bar{w}_{j\pm 1/2}^{n+1}$  and  $\bar{w}_j^{n+1}$  are reconstructed third-order piecewise polynomials [3] taken as

$$\begin{aligned} \bar{w}_{j\pm 1/2}^{n+1}(x) &= \tilde{A}_{j\pm 1/2} + \tilde{B}_{j\pm 1/2}(x - x_{j\pm 1/2}) \\ &\quad + \frac{1}{2} \tilde{C}_{j\pm 1/2}(x - x_{j\pm 1/2})^2, \\ \bar{w}_j^{n+1}(x) &\equiv \bar{w}_j^{n+1}, \end{aligned} \quad (13)$$

where the constants  $\tilde{A}_j$ ,  $\tilde{B}_j$  and  $\tilde{C}_j$  are evaluated as in [3]. The new cell averages on the unstaggered grids are obtained from these polynomials by [3]

$$\begin{aligned} \bar{u}_j^{n+1} &= \frac{1}{\Delta x} \left[ \int_{x_{j-1/2}}^{x_{j+1/2,L}} \bar{w}_{j-1/2}^{n+1} \, dx + \int_{x_{j+1/2,L}}^{x_{j+1/2,R}} \bar{w}_j^{n+1} \, dx \right. \\ &\quad \left. + \int_{x_{j+1/2,L}}^{x_{j+1/2,R}} \bar{w}_{j+1/2}^{n+1} \, dx \right]. \end{aligned} \quad (14)$$

The semi-discrete form is then defined by the limit

$$\frac{d\bar{u}_j(t)}{dt} = \lim_{\Delta t \rightarrow 0} \frac{\bar{u}_j^{n+1} - \bar{u}_j^n}{\Delta t}. \quad (15)$$

Proceeding with (13) and (14) as in [3], the coefficients in the polynomial form simplify resulting in

$$\begin{aligned} \frac{d\bar{u}_j}{dt} &= -\frac{1}{2\Delta x} [f(u_{j+1/2}^+(t)) + f(u_{j+1/2}^-(t)) \\ &\quad - f(u_{j-1/2}^+(t)) - f(u_{j-1/2}^-(t))] \\ &\quad - \frac{a_{j+1/2}(t)}{2\Delta x} [u_{j+1/2}^+(t) - u_{j+1/2}^-(t)] \\ &\quad - \frac{a_{j-1/2}(t)}{2\Delta x} [u_{j-1/2}^+(t) - u_{j-1/2}^-(t)] \\ &\quad + \lim_{\Delta t \rightarrow 0} \frac{1}{2\Delta x \Delta t} \int_{t^n}^{t^{n+1}} \int_{x_{j-1/2,L}}^{x_{j-1/2,R}} g \, dx \, dt \\ &\quad + \lim_{\Delta t \rightarrow 0} \frac{1}{2\Delta x \Delta t} \int_{t^n}^{t^{n+1}} \int_{x_{j+1/2,L}}^{x_{j+1/2,R}} g \, dx \, dt \\ &\quad + \lim_{\Delta t \rightarrow 0} \frac{1}{\Delta t (\Delta x - \Delta t (a_{j+1/2} + a_{j-1/2}))} \\ &\quad \times \int_{t^n}^{t^{n+1}} \int_{x_{j-1/2,R}}^{x_{j+1/2,L}} g \, dx \, dt. \end{aligned} \quad (16)$$

We note that the non-smooth parts of the solution are contained over spatial widths of size  $2a_{j\pm 1/2}^n \Delta t$ . Full details with clear sketches are given in [3]. Now, when the limits are taken on the source integrals, the first two vanish as the Riemann fans shrink to zero, since, for example:

$$x_{j+1/2,L} = x_{j+1/2} - a_{j+1/2} \Delta t \rightarrow x_{j+1/2}.$$

At the same time, since  $\bar{u}^n = \bar{u}(t)$  (and hence  $g$ ) is a constant over this cell, it can be shown for the other that

$$\begin{aligned} \lim_{\Delta t \rightarrow 0} \frac{1}{\Delta t (\Delta x - \Delta t (a_{j+1/2} + a_{j-1/2}))} \\ \times \int_{t^n}^{t^{n+1}} \int_{x_{j-1/2,R}}^{x_{j+1/2,L}} g \, dx \, dt = g(u_j^n). \end{aligned}$$

Hence the modified semi-discrete scheme with source term  $g(u(x, t))$  is

$$\begin{aligned} \frac{d\bar{u}_j}{dt} &= -\frac{1}{2\Delta x} [f(u_{j+1/2}^+(t)) + f(u_{j+1/2}^-(t)) \\ &\quad - f(u_{j-1/2}^+(t)) - f(u_{j-1/2}^-(t))] \\ &\quad - \frac{a_{j+1/2}(t)}{2\Delta x} [u_{j+1/2}^+(t) - u_{j+1/2}^-(t)] \\ &\quad - \frac{a_{j-1/2}(t)}{2\Delta x} [u_{j-1/2}^+(t) - u_{j-1/2}^-(t)] \\ &\quad + g(u_j(t)), \end{aligned} \quad (17)$$

where the rest of the terms are as in (3) and (4).

To compute with (17), it is convenient to use ODE system solvers, such as Runge–Kutta formulae. For instance, writing (17) in the form:

$$\frac{du_j}{dt} = F_j, \quad (18)$$

where  $F_j$  is the vector of the RHS, we can employ the second-order (in time) Runge–Kutta (RK2) or modified Euler scheme [8] for it as

$$\text{RK2} : \begin{cases} U^{(1)} = U^n + \Delta t F(U^n), \\ U^{(2)} = \frac{1}{2} U^n + \frac{1}{2} [U^{(1)} + \Delta t F(U^{(1)})], \\ U^{n+1} = U^{(2)}, \end{cases} \quad (19)$$

where  $U$  denotes the vector of components  $u_j$ , the superscript  $n$  and  $n + 1$  denote successive time levels, whilst the others (1, 2) denote intermediate values.

We shall refer to the scheme (17) with RK2 (19) as the SD3 scheme. We note that such a scheme is generally third order (in space) except in regions of steep gradients when it degrades to order two [3]. However, when the scheme is coupled with RK2, as here, the overall method is second order. It then makes sense when we compare its performance to that of the fully discrete second-order scheme (NNT) for systems with source terms for integration on unstaggered grids [4]:

$$\begin{aligned} \bar{u}_j^{n+1} = & \frac{1}{4}(\bar{u}_{j+1}^n + 2\bar{u}_j^n + \bar{u}_{j-1}^n) - \frac{1}{16}(u_{xj+1}^n - u_{xj-1}^n) \\ & - \frac{1}{8}[u_{xj+1/2}^{n+1} - u_{xj-1/2}^{n+1}] + \frac{1}{8}\Delta t[g(u_{j+1}^n) \\ & + 2g(u_j^n) + g(u_{j-1}^n)] + \frac{1}{8}\Delta t[g(u_{j+1}^{n+1}) \\ & + 2g(u_j^{n+1}) + g(u_{j-1}^{n+1})] - \frac{1}{4}\lambda[(f_{j+1}^n - f_{j-1}^n) \\ & + (f_{j+1}^{n+1} - f_{j-1}^{n+1})], \end{aligned} \tag{20}$$

where  $\lambda = \Delta t/\Delta x$  and the subscript  $x$  denotes differentiation with respect to  $x$ . This scheme has been obtained by modifying that of [1], following the prescription given in [5], but additionally taking into account a source term. Full details however, are left to another report [4]. Furthermore, we shall employ the scheme (20) in conjunction with the UNO derivative approximation [1]:

$$\begin{aligned} u_{xj} = & \text{MM}(u_j - u_{j-1} + \frac{1}{2}\text{MM}(u_j - 2u_{j-1} \\ & + u_{j-2}, u_{j+1} - 2u_j + u_{j-1}), \\ u_{j+1} - u_j = & \frac{1}{2}\text{MM}(u_{j+1} - 2u_j \\ & + u_{j-1}, u_{j+2} - 2u_{j+1} + u_j), \end{aligned} \tag{21}$$

where the function  $\text{MM}(\cdot)$  is the min-mod nonlinear limiter defined by

$$\text{MM}(s_1, s_2, \dots) = \begin{cases} \min\{s_j\} & \text{if } s_j > 0 \ \forall j, \\ \max\{s_j\} & \text{if } s_j < 0 \ \forall j, \\ 0 & \text{otherwise.} \end{cases} \tag{22}$$

2.2. Implementation details

The implementation of the NNT scheme (20) above follows previous reports [1,4], where in particular we mention that the source term can make the scheme implicit. The latter then requires fixed-point type iterations to convergence at each grid point at every time level.

The SD3 scheme is, however, explicit in time. Thus the implementation of (17) follows closely the prescription given in [3] where in particular we use for the non-oscillatory piece-wise polynomial (9) their CWENO reconstruction [3] given by

$$A_j = \bar{u}_j^n - \frac{1}{12}W_C(\bar{u}_{j+1}^n - 2\bar{u}_j^n + \bar{u}_{j-1}^n), \tag{23}$$

$$B_j = \frac{1}{\Delta x} \left[ W_R(\bar{u}_{j+1}^n - \bar{u}_j^n) + \frac{W_C}{2}(\bar{u}_{j+1}^n - \bar{u}_{j-1}^n) + W_L(\bar{u}_j^n - \bar{u}_{j-1}^n) \right], \tag{24}$$

$$C_j = \frac{W_C}{\Delta x^2}(\bar{u}_{j-1}^n - 2\bar{u}_j^n + \bar{u}_{j+1}^n). \tag{25}$$

Here the constants  $W_L, W_C$  and  $W_R$  are determined by their equation (2.9) and involve heuristic factors which have a bearing on the sharpness of the slopes near discontinuities.

In addition, it is required to compute at every time step the spectral radii (3) of the Jacobians of the flux terms, which we obtained exactly for the small test systems to follow.

3. Applications and tests

3.1. Shocks in a Broadwell gas

Here we solve the governing equations for a Broadwell gas [6,7]:

$$\frac{\partial \rho}{\partial t} + \frac{\partial m}{\partial x} = 0, \tag{26}$$

$$\frac{\partial m}{\partial t} + \frac{\partial z}{\partial x} = 0, \tag{27}$$

$$\frac{\partial z}{\partial t} + \frac{\partial m}{\partial x} = \frac{1}{\varepsilon}(\rho^2 + m^2 - 2\rho z), \tag{28}$$

where  $\varepsilon$  is the mean free path and  $\rho(x, t), u(x, t), m(x, t) \equiv \rho(x, t)u(x, t), z(x, t)$  the density, flow velocity, momentum and flux, respectively. The range  $\varepsilon = 1 \dots 10^{-8}$  cover the regime from the non-stiff to the highly stiff. In particular, the limit  $\varepsilon = 10^{-8}$  requires a renormalization of the variables such as in the form

$$\bar{x} = \frac{1}{\varepsilon}x, \quad \bar{t} = \frac{1}{\varepsilon}t$$

followed by computations on an equivalent finer grid (see, for example, [9]).

We observe that in the limit  $\varepsilon \rightarrow 0$  we arrive at

$$z = z_E(\rho, m) = \frac{1}{2\rho}(\rho^2 + m^2), \tag{29}$$

which leads to the equilibrium solution of the governing equations above which then reduce to the Euler equations.

The SD3 (17) and NNT (20) schemes were applied to the above with the two sets (*Rim1* and *Rim2*) of initial conditions (applied at  $t = 0$ ) corresponding to several Riemann problems, each distinguished by a specific  $\varepsilon$ -value:

$$\begin{aligned} \text{Rim1} : & \begin{cases} \rho = 2, m = 1, z = 1, & x < x_J, \\ \rho = 1, m = 0.13962, z = 1, & x > x_J, \end{cases} \\ \text{Rim2} : & \begin{cases} \rho = 1, m = 0, z = 1, & x < x_J, \\ \rho = 0.2, m = 0, z = 1, & x > x_J. \end{cases} \end{aligned}$$

In all calculations absorbing boundary conditions were employed, where in particular, the boundary values were obtained by quadratic extrapolations of internal point values on a fixed spatial grid, over an integration domain on the  $X$ -axis. Results obtained are depicted in Fig. 1.

Other parameters used here were  $\Delta x = 0.01$ ,  $\Delta t = 0.005$ ,  $x_J = 5$  in (a) and (b) and  $\Delta x = 0.02$ ,  $\Delta t = 0.001$ ,  $x_J = 10$  in (c) and (d) for both methods. We observe that in virtually all cases, the semi-discrete scheme gives better results than the modified NNT scheme.

### 3.2. Shocks in an Eulerian gas with heat transfer

Here we solve the Euler equations for the one-dimensional flow of a gas in contact with a constant temperature bath [10]:

$$\begin{aligned} \frac{\partial \rho}{\partial t} + \frac{\partial(\rho u)}{\partial x} &= 0, & \frac{\partial(\rho u)}{\partial t} + \frac{\partial(\rho u^2 + p)}{\partial x} &= 0, \\ \frac{\partial(\rho E)}{\partial t} + \frac{\partial(\rho u E + up)}{\partial x} &= -K\rho(T - T_0). \end{aligned}$$

The  $\rho, u, e, T, E = e + (1/2)u^2$  and  $p = (\gamma - 1)\rho e$  are the density, flow velocity, internal energy, temperature in units of  $e$ , total energy and pressure, respectively,

with  $K > 0$  the heat transfer coefficient and  $T_0$  the constant bath temperature, taken as 1 (i.e.  $e$  as in [10]).

The initial conditions (at  $t = 0$ ) used were

$$\text{Rim3} : \begin{cases} \rho = 2.5, u = 1.0, p = 1.0, & x < 50, \\ \rho = 1.0, u = 0.4, p = 0.4, & x > 50, \end{cases}$$

where different  $K = 1, 50, 400, 1000$  are employed. Computed results with SD3 and NNT are shown in Fig. 2.

In these we observe that SD3 captures the shocks significantly better than does NNT. The oscillations seen in the small and large  $K$  regimes have also been observed by Pember [10], employing a Godunov type frozen characteristic method. In his study it was found that when the actual wave speed lies closer to the equilibrium ( $\sim K \rightarrow \infty, T \rightarrow T_0$ ) characteristic speed or lies closer to the frozen ( $\sim K \rightarrow 0$ ) characteristic speed then an ambiguity can arise in the use of the full set of model equations with  $0 < K < \infty$ . This causes the relaxation times at either ends to tend to become non-resolvable, resulting in non-physical oscillations near discontinuities. In comparison, we observe that the NNT curves generally show poor resolution of the shocks, and moreover far more dissipation, as expected when  $\Delta t \sim (\Delta x)^2$  [3].

### 3.3. Convergence rates and complexity

It is of interest to compare the methods in terms of their relative convergence rates and complexities. For the former exercise we employed as a test problem the Broadwell equations (26)–(28) with  $\varepsilon = 1$  and computed smooth solutions corresponding to the same boundary conditions and the initial conditions:

$$\begin{aligned} \rho(x, 0) &= 1 + a_\rho \sin \frac{2\pi x}{L}, \\ u(x, 0) &= \frac{1}{2} + a_\rho \sin \frac{2\pi x}{L}, \\ m(x, 0) &= \rho(x, 0)u(x, 0), \\ z(x, 0) &= 0.2z_E(\rho(x, 0), m(x, 0)), \end{aligned} \tag{30}$$

where  $z_E$  is given by (29) and  $L = 20, a_\rho = 0.3, a_v = 0.1, \Delta t/\Delta x = 5/6$  with the final time set to  $T = 5$ .

We employed successively the number of grid points  $N = 100, 200, 400$  and took the refined

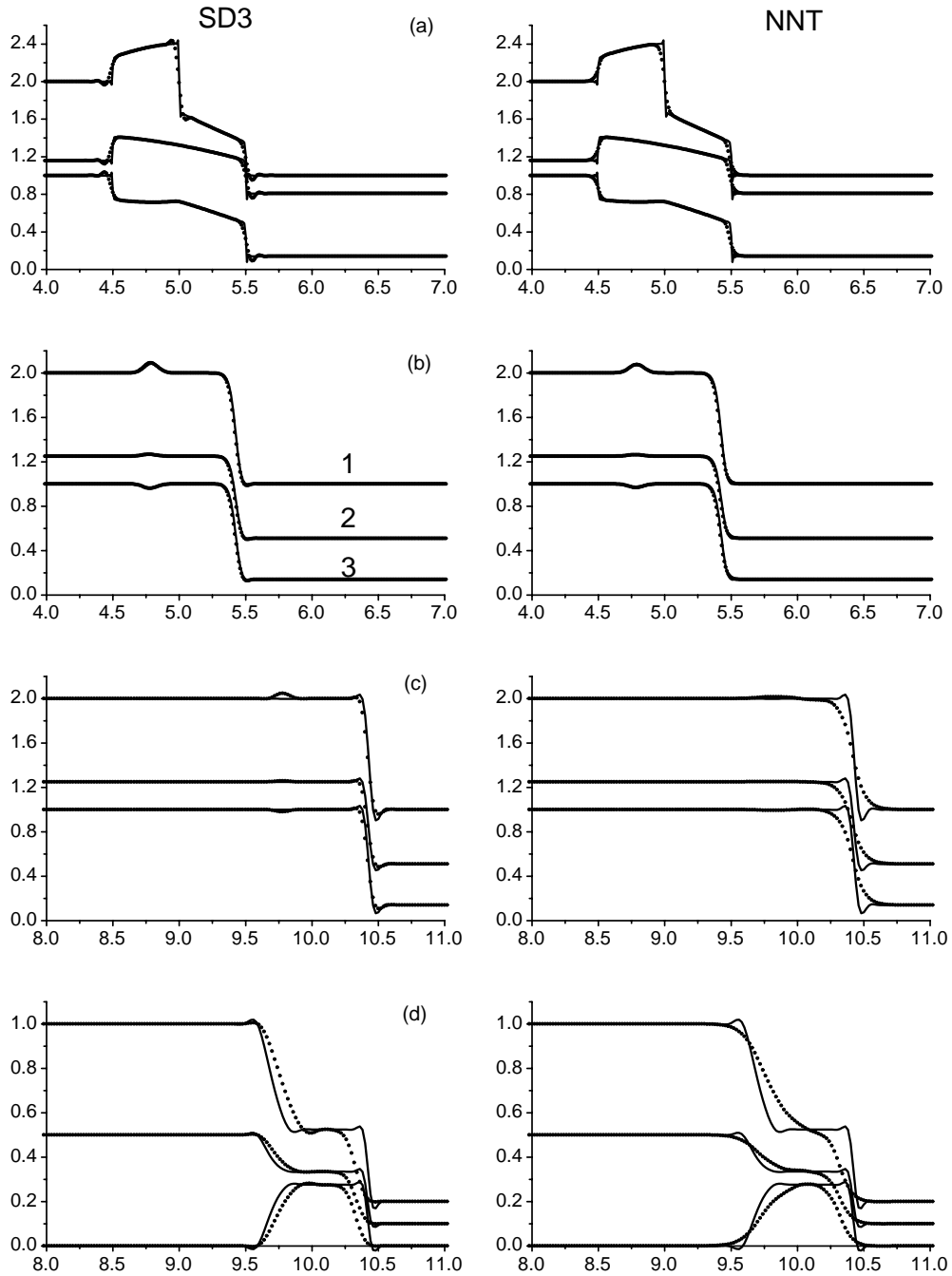


Fig. 1. Broadwell gas shock solutions with: (a)  $\varepsilon = 1$  (*Rim1*); (b)  $\varepsilon = 0.02$  (*Rim1*); (c)  $\varepsilon = 10^{-8}$  (*Rim1*); (d)  $\varepsilon = 10^{-8}$  (*Rim2*). Here the curve labeled  $1 \sim \rho$ ,  $2 \sim z$ ,  $3 \sim m$ . The snapshot time is  $t = 0.5$  in all cases. The heavy lines are computed solutions and the thin lines are 'exact' or refined grid solutions obtained by reducing the time and space steps by a factor of 10.

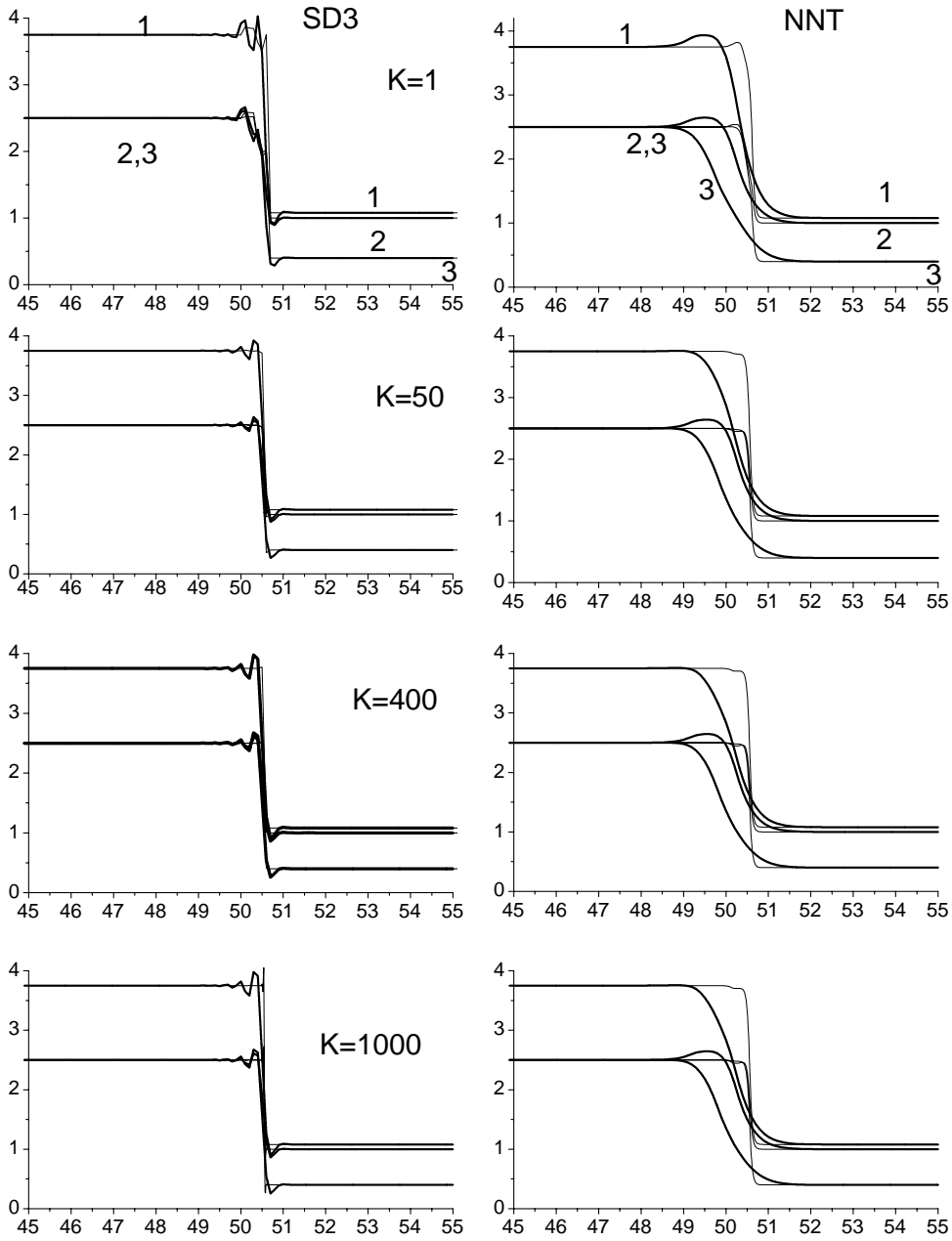


Fig. 2. Shocks in an Eulerian gas with heat transfer. The curve labeled  $1 \sim \rho E, 2 \sim \rho, 3 \sim \rho u$ . The grid lengths of  $\Delta x = 0.1$  and  $\Delta t = 0.001$  were used for both methods. The output time is  $t = 0.4$  in all cases. Again the heavy lines are computed solutions and the thin lines are 'exact' solutions, obtained as for Fig. 1.

Table 1  
Convergence rates for the NNT and SD3 schemes

$N$	$L^\infty$ error	$CR_i$
NNT		
100	0.151188	–
200	0.023043	2.72
400	0.0055693	2.06
SD3		
100	0.114549	–
200	0.015966	2.85
400	0.001880	3.10

Table 2  
CPU times (s) for the NNT and SD3 schemes

$N$	NNT	SD3
100	0.11	0.17
200	0.33	0.38
400	1.10	1.15
800	3.63	3.90

(exact) solution as that given by  $N = 800$ . Then the convergence rate ( $CR_i$ ) was computed by the formula

$$CR_i = \frac{\log(\text{error}_i/\text{error}_{i+1})}{\log(\Delta x_i/\Delta x_{i+1})}, \quad (31)$$

where  $\text{error}_i$ , for example, is the absolute  $L^\infty$  norm error corresponding to the refinement  $i$ . For both methods the results are displayed in Table 1.

We observe that the SD3 scheme, for larger  $N$ , tends to approach a third-order scheme, whilst the NNT is clearly second-order, as expected.

As far as the complexities of the two schemes are concerned, we computed the CPU times for the same problem given above with results depicted in Table 2. We observe that SD3 takes some 8–10% more computation time than NNT for larger problems. This is in spite of the explicit nature of SD3. We attribute the larger times to the CWENO construction (23)–(25) as well as the Runge–Kutta function updates in (19). For the NNT, although implicit in time, we find rapid convergence (2–3 iterations only). A significant amount of time here is spent on UNO derivative calculations (21) required in (20), which in contrast are not required explicitly in SD3.

## 4. Conclusion

We have indicated in this work, how the third-order semi-discrete numerical scheme of Kurganov and Levy [3] can be suitably adapted to include source terms in one-dimensional hyperbolic systems. Results obtained with it on shock propagation in a Broadwell gas and in a gas dynamics model with heat transfer show that in some cases it performs better than the fully discrete modification for systems with source terms [4]. In others, their accuracies are similar. Further, whilst the convergence rate for the explicit Kurganov–Levy scheme is superior to the implicit NNT scheme, it has been shown to be around 10% more computationally expensive than the NNT scheme for problems on moderate to large size grids.

## Acknowledgements

The authors wish to thank Professors D. Levy, G. Russo and Shi Jin for their helpful correspondences. They are also grateful to the referees for their constructive criticisms.

## References

- [1] H. Nessyahu, E. Tadmor, Non-oscillatory central differencing for hyperbolic conservation laws, *J. Comput. Phys.* 87 (1990) 408–463.
- [2] A. Kurganov, E. Tadmor, New high-resolution central schemes for nonlinear conservation laws and convection–diffusion equations, *J. Comput. Phys.* 160 (2000) 241–282.
- [3] A. Kurganov, D. Levy, A third-order semi-discrete central scheme for conservation laws and convection–diffusion equations, *SIAM J. Sci. Comput.* 22 (2000) 1461–1488.
- [4] R. Naidoo, S. Baboolal, Numerical integration of the plasma fluid equations with a non-staggered modification of the second-order Nessyahu–Tadmor central scheme and soliton modelling, *Math. Comput. Simul.*, Special Issue on Nonlinear Waves, submitted.
- [5] G.-S. Jiang, D. Levy, C.-T. Lin, S. Osher, E. Tadmor, High-resolution non-oscillatory central schemes with non-staggered grids for hyperbolic conservation laws, *SIAM J. Numer. Anal.* 35 (1998) 2147–2168.
- [6] R.E. Caflisch, S. Jin, G. Russo, Uniformly accurate schemes for hyperbolic systems with relaxation, *SIAM J. Numer. Anal.* 34 (1997) 246–281.
- [7] S. Jin, Runge–Kutta methods for hyperbolic conservation laws with stiff relaxation terms, *J. Comput. Phys.* 122 (1995) 51–67.

- [8] J. Stoer. R. Bulirsch, *Introduction to Numerical Analysis*, Springer, New York, 1980, p. 414.
- [9] G. Naldi, L. Pareschi, Numerical schemes for hyperbolic systems of conservation laws with stiff diffusive relaxation, *SIAM J. Numer. Anal.* 37 (2000) 1246–1270.
- [10] R.B. Pember, Numerical methods for hyperbolic conservation laws with stiff relaxation. II. Higher-order Godunov methods, *SIAM J. Sci. Comput.* 14 (1993) 824–829.



**R. Naidoo** obtained the BSc (Hons) degree in Applied Mathematics from the University of Durban-Westville in 1990 and the MSc degree in Mathematical Studies from the University of Western Cape in 1996. He holds the position of Lecturer in the Department of Mathematics and Physics at the Durban Institute of Technology and is completing the PhD degree in the School of Mathematical Sciences, Information Technology and Computer Science at the University of Durban-Westville.



**S. Baboolal** obtained the BSc (Hons)/MSc degrees in Physics in 1972/1975 from the University of Durban-Westville, the MSc degree in Numerical Analysis in 1980 from the University of Dundee and the PhD degree in Theoretical and Computational Plasma Physics from the University of Natal in 1989. He has held positions of Senior Lecturer in Mathematics and

Applied Mathematics, Assistant Director of Academic Computer Services, Senior Lecturer and then Associate Professor in Computer Science in the School of Mathematical Sciences, Information Technology and Computer Science at the University of Durban-Westville. His research interests lie mainly in numerical methods, modeling of plasma nonlinearities and scientific software.